No-Core MCSM calculation for ^{10}Be and ^{12}Be low-lying spectra

Lang Liu*
Department of Physics, University of Tokyo, Hongo, Tokyo 113-0033, Japan
State key Laboratory of Nuclear Physics and Technology,
School of Physics, Peking University, Beijing 100871, P. R. China

Takaharu Otsuka
Department of Physics, University of Tokyo, Hongo, Tokyo 113-0033, Japan
Center for Nuclear Study, University of Tokyo, Hongo, Tokyo 113-0033, Japan
National Superconducting Cyclotron Laboratory, Michigan State University, East Lansing, Michigan, 48824, USA

Noritaka Shimizu
Department of Physics, University of Tokyo, Hongo, Tokyo 113-0033, Japan

Yutaka Utsuno
Japan Atomic Energy Agency, Tokai, Ibaraki, 319-1195 Japan

Robert Roth
Institut für Kernphysik, Technische Universität Darmstadt, D-64289 Darmstadt, Germany
(Dated: July 4, 2012)

The low-lying excited states of ^{10}Be and ^{12}Be are investigated within a no-core Monte Carlo Shell Model (MCSM) framework employing a realistic potential obtained via the Unitary Correlation Operator Method. The excitation energies of the 2^+_1 and 2^+_2 states and the B(E2; $2^+_{1,2} \rightarrow 0^+_{g.s.}$) for ^{10}Be in the MCSM with a standard treatment of spurious center-of-mass motion show good agreement with experimental data. Some properties of low-lying states of ^{10}Be are studied in terms of quadrupole moments, E2 transitions and single-particle occupation numbers. The E2 transition probability of ^{10}C, the mirror nucleus of ^{10}Be, is also presented with a good agreement to experiment. The triaxial deformation of ^{10}Be and ^{10}C is discussed in terms of the B(E2) values. The removal of the spurious center-of-mass motion affects differently on various states: for instance, negligible effects on the 2^+_1 and 2^+_2 levels of ^{10}Be, while significant and favorable shift for the 1^-_1 level. It is suggested that the description of ^{12}Be needs a larger model space as well as some other higher excited states of ^{10}Be, as an indicator that these are dominated by intruder configurations.

PACS numbers: 21.60.Cs,21.60.De,21.60.Ka,27.20.+n

I. INTRODUCTION

One of the major goals in nuclear physics is to understand the structure and reactions of nuclei starting from realistic nuclear interactions. Besides the challenge of solving the nuclear many-body problem, this endeavor is complicated by the fact that our understanding of the nuclear force is not complete yet. At present, there are two ways to construct an accurate representation of nuclear force. One can construct a two-body potential phenomenologically by fitting experimental data on nucleon-nucleon (NN) scattering, as it is done in the Argonne V18 potential [1], the CD-Bonn potential [2] and the Nijmegen potentials [3]. Alternatively, consistent two- and many-body interactions can be constructed in the framework of chiral effective field theory using the symmetries and the effective degrees of freedom of low-energy QCD as a guiding principle. The chiral N^{3}LO potential is such an accurate charge-dependent nucleon-nucleon potential constructed at fourth order of chiral perturbation theory [4–6]. By using these realistic nuclear interactions, *ab initio* nuclear many-body calculations have been performed in the last decade. In Green's Function Monte Carlo (GFMC) calculations the exact ground-state wave function is calculated by treating the many-body Green's functions in a Monte Carlo approach [7–9]. The GFMC calculations of light nuclei up to ^{12}C with the Argonne interaction reproduce the experimental nuclear binding energies and radii as well as the spectra. Another *ab initio* approach for nuclei up to A=14 is the No-Core Shell Model (NCSM) [10–12]. All nucleons are treated in a large number of shell-model basis, providing similarly successful description of light nuclei.

However, the straightforward application of those realistic interactions in nuclear many-body calculations is still difficult due to the strong short-range repulsion which generates strong correlations in the nuclear many-body state. The Unitary Correlation Operator Method (UCOM) is one of the methods to tackle this problem by introducing a unitary transformation such that the transformed many-body states contain the information on the dominant correlations in nuclear many-body system [13–

* liulang@pku.edu.cn

15]. In the UCOM approach two unitary transformation operators are defined, a central correlation operator and a tensor correlation operator, which correspond to two most important correlations: the central correlations induced by the strong short-range repulsion and the tensor correlations, respectively. Through a unitary transformation of the Hamiltonian, a soft phase-shift equivalent two-nucleon interaction can be obtained. This UCOM potential can be used in various kinds of many-body calculations, such as no-core shell model calculations [16–19].

In the shell model calculations, the direct diagonalization of the Hamiltonian matrix in the full valence-nucleon Hilbert space is difficult, as the dimension of such a space becomes larger and larger when one moves from light nuclei to heavier nuclei. Much effort of truncation frameworks to full shell-model calculation has been directed, e.g. in Refs [16, 20, 21]. As another way to overcome this difficulty, the stochastic approaches have been introduced. Among them, the Shell Model Monte Carlo (SMMC) method has been successfully proposed [22]. Nevertheless, the SMMC is basically suitable for the ground state and thermal properties, and suffers from the so-called "sign problem". As a completely different approach, the Quantum Monte Carlo Diagonalization (QMCD) method has been proposed for solving quantum many-body systems with a two-body interaction [23–26]. The QMCD can describe not only the ground state but also excited states, including their energies, wave functions and hence transition matrix elements.Thus, on the basis of the QMCD method, the Monte Carlo Shell Model (MCSM) has been introduced [27] for nuclear shell model calculations [28–32]. An extrapolation method in the Monte Carlo Shell Model has been proposed very recently [33]. The applicability of the MCSM to a system beyond the current limit of exact diagonalization is shown for the $pf + g_{9/2}$-shell calculation by assuming a core in their work. It is then of a certain importance and interest to apply the MCSM to *ab initio* calculations of light nuclei. As the MCSM has never been used in *ab initio* calculations, we start with straightforward calculations by taking conventional MCSM method and code which have been used for many shell-model calculations for medium-mass nuclei. We shall present, in this paper, how such *ab initio* calculations work. We note that the MCSM method is being revised in parallel, and outlines of such revisions and future directions can be found in Refs. [34, 35]. The results to be shown in this paper will play a key role in judging as to whether one should move ahead to more systematic calculations with the revised method or not.

The MCSM calculation is performed without a core to make it *ab initio*. In Section 2, we will introduce the theoretical framework of the MCSM and explain the general procedure of the Monte Carlo Shell Model method. ^{4}He, which is investigated in the framework of the shell model and the MCSM by using the UCOM potential, is discussed in Section 3 as the numerical check. Study of structure and low lying spectra for Beryllium isotopes appears in Section 4. In Section 5, the conclusion with a summary and description of future direction for research in this field is given.

II. MONTE CARLO SHELL MODEL CALCULATION

The main idea of the MCSM is to diagonalize the Hamiltonian in a subspace spanned by the MCSM basis states, which are generated in a stochastic way.

We begin with the imaginary-time evolution operator

$$e^{-\beta H}, \tag{1}$$

where H is a given general (time-independent) Hamiltonian and $\beta \propto T^{-1}$ is a real number with T being analogous to a temperature. If this operator in Eq. (1) acts on a state $|\Psi^{(0)}\rangle$, one obtains

$$e^{-\beta H}|\Psi^{(0)}\rangle \;=\; \sum_i e^{-\beta E_i} c_i |\psi_i\rangle, \tag{2}$$

where E_i is the i-th eigenvalue of H, $|\psi_i\rangle$ is the corresponding eigenstate and c_i its amplitude in the initial state:

$$|\Psi^{(0)}\rangle \;=\; \sum_i c_i |\psi_i\rangle. \tag{3}$$

For β large enough, only the ground and low-lying states survive. But the actual handling is very complicated for H containing a two-body (or many-body) interaction.

The Hubbard-Stratonovich (HS) transformation [36, 37] can be used to ease the difficulty mentioned above. We then move to the formula

$$|\Phi(\sigma)\rangle \;\propto\; e^{-\beta h(\sigma)}|\Psi^{(0)}\rangle, \tag{4}$$

where $h(\sigma)$ is a one-body Hamiltonian obtained through the HS-transformation and σ is a set of random numbers (auxiliary fields). The right-hand-side of this relation can be interpreted as a means to generate all basis vectors needed for describing the ground state and the low-lying states. For different values of the random variable, σ, one obtains different state vectors, $|\Phi(\sigma)\rangle$, by Eq. (4). These vectors are labeled as candidate states and selected as MCSM basis by a procedure of energy comparison [27].

During the MCSM generation of the basis vectors, symmetries, e.g. rotational and parity symmetry, are restored before the diagonalization as more basis vectors are included. All MCSM basis states are projected onto good parity and angular momentum quantum numbers by acting with the corresponding projection operators. We diagonalize the Hamiltonian in a subspace spanned by those projected basis vectors. The number of the MCSM basis states is referred to as the MCSM dimension. The basis generation process for general cases is outlined in Ref. [27].

As more than one major shell is included in the MCSM calculation, the spurious center-of-mass motion must be

accounted for. The Lawson's prescription is adopted to suppress the spurious center-of-mass motion in good approximation for major shell truncation [38]. The total Hamiltonian then consists of intrinsic and center-of-mass parts as,

$$H' = H_{int.} + \beta_{c.m.} H_{c.m.}, \tag{5}$$

where $H_{int.}$ is the intrinsic Hamiltonian. The $H_{c.m.}$ is defined by

$$H_{c.m.} = \frac{\mathbf{P}^2}{2AM} + \frac{1}{2} M A \omega^2 \mathbf{R}^2 - \frac{3}{2}\hbar\omega, \tag{6}$$

where $\mathbf{R}$ and $\mathbf{P}$ are the coordinate and momentum of the center of mass, respectively. In general, by taking sufficiently large values of $\beta_{c.m.}$, spurious components are suppressed for the low-lying eigenstates of H'.

III. RESULTS FOR ^{4}He

In this section we discuss the interactions and model spaces used for the no-core MCSM and provide some benchmark calculations for the ^{4}He ground state. The model space of the MCSM is spanned by a harmonic oscillator basis truncated with respect to the unperturbed single-particle energies $e_{\max} = 2n + l$. We use UCOM-transformed realistic two-nucleon interactions as input potential. In addition to the standard UCOM interaction derived from the Argonne V18 potential, which has been used in a series of applications in various many-body methods [15], we adopt a new UCOM potential based on the chiral N^{3}LO two-nucleon interaction of Entem and Machleidt [4, 6]. These UCOM potentials are labeled as $V_{\rm UCOM}$(AV18) and $V_{\rm UCOM}$(N^{3}LO), respectively. In both cases the UCOM correlation functions are determined through an energy minimization in the two-nucleon system with a constraint on the range of the even spin-triplet tensor correlator [15]. We neglect Coulomb interaction in all of our calculations throughout this work for simplicity.

As an example of the UCOM potential, we perform a straightforward shell model diagonalization within a harmonic oscillator basis without a core. In this shell model calculation, we employ the NuShell code developed by B.A. Brown *et al.* [39] and use the $V_{\rm UCOM}$(N^{3}LO) potential.

The ground-state energy for ^{4}He as a function of the harmonic oscillator frequency $\hbar\omega$ in various model spaces characterized by the oscillator basis cut off parameter $e_{\max}$, is shown in Fig. 1. The shell-model description of many-body correlations depends in general on the size of the model space. The experimental value is shown as a black line. The ground-state energy for small model spaces, e.g., $e_{\max}$=2, shows a sizable dependence on $\hbar\omega$. By increasing the size of the model space, the ground-state energy is lowered and dependence on $\hbar\omega$ is reduced. The ground-state energy varies by about 1 MeV for a range of oscillator frequencies $\hbar\omega$ from 24 MeV to 52 MeV. There is still about 1 MeV difference between

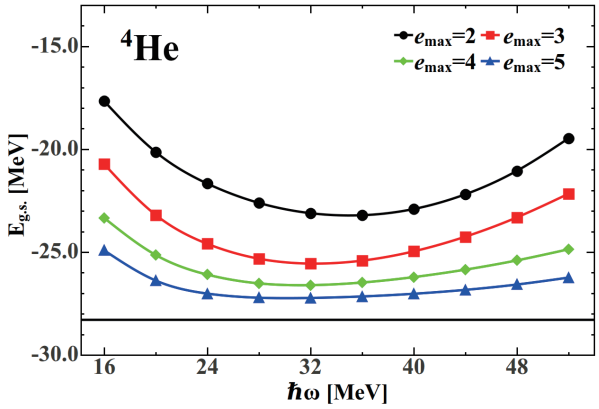

FIG. 1. (Color online) The ground-state energy of ^{4}He as a function of harmonic oscillator frequency $\hbar\omega$ in different model spaces ($e_{\max}$ from 2 to 5) calculated in NuShell using the $V_{\rm UCOM}$(N^{3}LO) potential. The symbols correspond to $e_{\max}$ from 2 to 5. The straight line is experimental value.

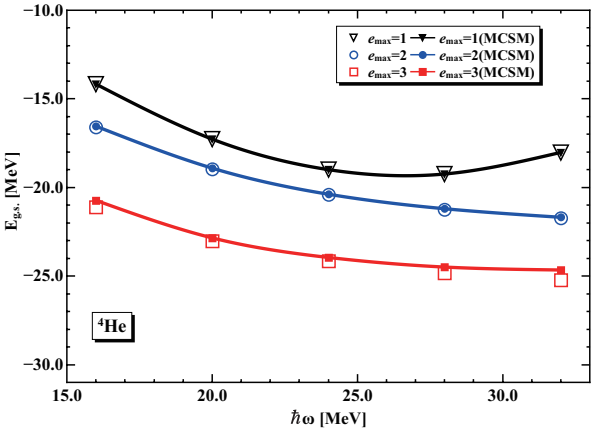

FIG. 2. (Color online) The ground-state energy of ^{4}He as a function of the harmonic oscillator parameter $\hbar\omega$ using UCOM potential $V_{\rm UCOM}$(AV18) in $e_{\max}$=1 (black), 2 (blue), and 3 (red) model space. The open symbols indicate results by the conventional direct diagonalization method in the m-scheme. The closed symbols indicate the MCSM results.

the $e_{\max}$=5 result at $\hbar\omega$=32 MeV and the experimental ground-state energy. Evidently, still larger values of $e_{\max}$ are needed to reproduce the experimental binding energy of ^{4}He, which the $V_{\rm UCOM}$(N^{3}LO) interaction is approximately adjusted to. At present, the conventional shell model calculation is performed only up to $e_{\max} = 5$ model space due to the limitation of Nushell code. However, the convergence is significantly better than for the bare realistic nucleon-nucleon potential. The comparison between bare interaction and the UCOM interaction in the shell model calculation for ^{4}He can be found in Ref. [40].

We now compare the full shell-model and the MCSM results for the ground-state energy of ^{4}He using the $V_{\rm UCOM}$(AV18) potential. Figure 2 shows the ground-

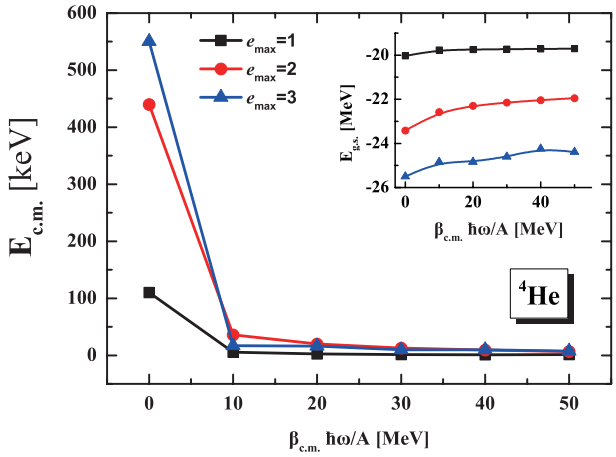

FIG. 3. The center-of-mass motion energy and the ground-state energy (inset) of ^{4}He as a function of Lawson's prescription parameter $\beta_{c.m.}$ defined in eq. (5). The model spaces are $e_{\max}$=1, 2 and 3. The oscillator parameter $\hbar\omega$ is 28 MeV. The potential $V_{\rm UCOM}$(N^{3}LO) is used.

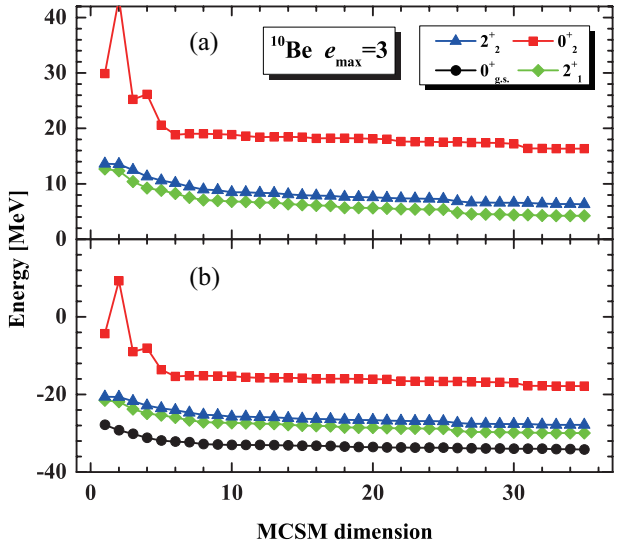

FIG. 4. (Color online) (a) Excitation energies of the 2^+_1 state (green diamonds), the 2^+_2 state (blue triangles) and the 0^+_2 state (red squares) as functions of the MCSM dimension in the $e_{\max}$ = 3 space. (b) Energies of the states shown in (a) as well as the 0^+_1 (ground) state (black circles). $\beta_{c.m.} \cdot \hbar\omega/A$ = 10 MeV is used to remove spurious components.

state energy for ^{4}He for both calculations as a function of the oscillator frequency $\hbar\omega$ in small model spaces ($e_{\max}$=1, 2 and 3). The MCSM results obtained with 32∼50 MCSM dimensions are in reasonable agreement with the results from a full diagonalization in these model spaces.

The treatment of spurious center-of-mass motion of ^{4}He is illustrated in Fig. 3. Figure 3 shows the dependence of the expectation value of $H_{c.m.}$ and the ground-state energy (inset) obtained with Lawson's prescription parameter $\beta_{c.m.}$ in the $e_{\max}$=1, 2 and 3 model spaces. The expectation value of $H_{c.m.}$ decreases rapidly and reaches a converged small value. In this way, the spurious center-of-mass motion can be suppressed to a large extent by choosing a suitable $\beta_{c.m.}$ value.

IV. LOW LYING SPECTRA OF ^{10}Be AND ^{12}Be

The ^{10}Be nucleus is a good candidate for testing *ab initio* calculations employing realistic nuclear interactions, as there are adequate experimental data both in the ground state and in the excited states, e.g., excitation energies of two J^π=2$^+$, T=1 states and the $B(E2)$ value of those states to the ground state. The AMD calculations of Be isotopes [41], the GFMC approach [7, 8] and the NCSM [11, 42] have been used to investigate p-shell nuclei like ^{10}Be and to reproduce features such as binding energies and excitation spectra. This work is a new attempt to investigate these states by applying the no-core MCSM with realistic nuclear interactions. In this section, we present MCSM results for ^{10}Be and ^{12}Be.

We discuss MCSM calculations using $V_{\rm UCOM}$(N^{3}LO) potential in an $e_{\max}$=3 model space. For the beryllium isotopes, the ground-state energies exhibit a minimum for oscillator frequencies $\hbar\omega$ around 16.0 MeV in the conventional shell model calculation [43]. We use bare charges, hence the electric quadrupole moment is equal to the proton quadrupole moment.

For a more precise investigation, we have to remove spurious components with respect to the center-of-mass motion, if they are mixed in calculated eigenfunctions. As discussed earlier, we use Lawson's prescription with a suitably chosen $\beta_{c.m.}$ in eq. (5). We shall use $\beta_{c.m.} \cdot \hbar\omega/A$ = 10 MeV hereafter, unless otherwise specified. The same value has been taken in many MCSM calculations (not of *ab initio* type), *e.g.*, [29].

The convergence of low-lying excitation energies as a function of the MCSM dimension has to be examined, as our goal is to investigate the excitation spectra. Figure 4 (a) shows the excitation energies of the 2^+_1, 2^+_2 and 0^+_2 states as functions of the MCSM dimension for the $e_{\max}$=3 model space. If we evaluate the energy difference ϵ between results corresponding to the last two consecutive MCSM dimensions, we obtain ϵ=18 keV for 2^+_1, 15 keV for 2^+_2 and 37 keV for 0^+_2. The relative accuracy of these excitation energies is $\sim$ 0.3% for 2$^+$ states and $\sim$ 0.7% for 0^+_2 state. In the MCSM calculation, the diagonalization is performed in a subspace comprised of 25 to 50 optimally generated basis states. The size (dimension) of this subspace is quite small compared to that of the entire Hilbert space taken in the direct diagonalization in the conventional shell model. This advantage will be even more obvious for heavier nuclei by the fact that the full diagonalization in $e_{\max}$ = 3 is hardly feasible with other calculational techniques available presently.

Figure 4 (b) exhibits the energies of the $0^+_{1,2}$ and $2^+_{1,2}$ states as functions of the MCSM dimension. One sees

steady improvements of these energies, particularly for the dimension greater than 30. The energies appear to become converged to a rather good extent. Figure 4 (b) shows that the ground-state energy becomes about -35 MeV for dimensions large enough. This is still far from the experimental value $\sim$ -65 MeV. After the Coulomb correction $\sim$ 5 MeV, the difference is $\sim$ 35 MeV, which is in part due to the choice of the interaction where three-body forces are missing. The model space and the convergence also contribute to the discrepancy. Such problems are important issues in present and future MCSM projects. On the other hand, the present calculation appears to be rather reasonable for excitation energies as shown later, and we use the $V_{\rm UCOM}(\rm N^3LO)$ potential in this first attempt.

We now discuss properties of the 0^+_1 and $2^+_{1,2}$ states of ^{10}Be. Figure 5 shows energy levels of these states. Some other low-lying states of ^{10}Be are shown also, and will be discussed later. While the MCSM results are about 1 MeV and 0.6 MeV higher than the experimental values for 2^+_1 and 2^+_2, respectively, the basic patterns and scale are reproduced well by the MCSM calculation. In particular, the low-lying 2^+_2 level is a characteristic indicator of triaxial deformation, as discussed later.

We now investigate these excited states in terms of the quadrupole moments, E2 transitions and occupation probabilities. The quadrupole moments of protons and neutrons for the 2^+_1 and 2^+_2 states of ^{10}Be are shown, respectively, in Fig. 6. One finds that beyond MCSM dimension of 30, those quadrupole moments reach stable values. The nucleus ^{10}Be has a negative quadrupole moment for the 2^+_1 state. In contrast, the 2^+_2 state shows a positive quadrupole moment. These features are also predicted in Ref. [1]. We note that the protons have stronger deformation than neutrons in both states of ^{10}Be, because there are two valence protons and four valence neutrons in the p-shell in major configurations, and the former produce stronger deformation than the latter.

The B(E2) values from the $2^+_{1,2}$ states to the ground state of ^{10}Be are shown in Table I, in comparison to results by NCSM [11, 44], GFMC [44], and AMD [41]. The present result is rather similar to the CDB2k NCSM results among those shown in this table.

Some B(E2) values are calculated also for the mirror nucleus, ^{10}C, in the isospin formalism, as shown in Table II. This table indicates that MCSM value of $\mathrm{B(E2}; 2^+_1 \rightarrow 0^+_{g.s.})$ appears to be in rather good agreement with the corresponding experimental data [44, 45] for both ^{10}Be and ^{10}C. This is of certain importance because from the viewpoint of the liquid-drop model, B(E2) value is proportional to Z^2, and thereby the value of ^{10}C is expected to be larger than the corresponding one of ^{10}Be, by a factor of $6^2/4^2$ in a naive expectation. While we take only bare charge ($e_p = e$ and $e_n = 0$ with e being the unit charge), we can still produce almost the same values of $\mathrm{B(E2}; 2^+_1 \rightarrow 0^+_{g.s.})$ of ^{10}Be and ^{10}C. This is because although there are two more protons in ^{10}C than in ^{10}Be, they do not necessarily increase quadrupole deformation, partly due to the $0p_{3/2}$ closed-shell formation.

We note that the $\mathrm{B(E2}; 2^+_1 \rightarrow 0^+_{g.s.})$ value for ^{10}C has been obtained by NCSM calculations as 5.702 e^2 fm^4 [11] and 10 ± 2 e^2 fm^4 [46]. A GFMC value has been reported as 15.3 (1.4) e^2 fm^4 [44]. The present value, 9.3 e^2 fm^4, appears to be the closest to the observed value.

The MCSM value of the spectroscopic quadrupole moment of the 2^+_1 state of ^{10}C is obtained also from Fig. 6 as 3.04 e fm^2 by exchanging proton and neutron.

The nuclei ^{10}C and ^{10}Be belong to the same isospin multiplet of T=1. In the notation of Timmer [47], which makes direct use of the isospin formalism, one may write the E2 strength as

$$B(E2) = [(e_p + e_n)S + T_z(e_p - e_n)V]^2, \qquad (7)$$

where the e_p and e_n are the effective charges being $e_p = e$ and $e_n = 0$ in the present work. The reduced isoscalar and isovector matrix elements S and V must either be determined from experiment or be calculated with the help of suitable model wave functions. In Ref. [48], the B(E2) value is proportional to $[3.2 + 0.1 \times T_z]^2$. The B(E2) value of ^{10}C should then be smaller than that in ^{10}Be, as $T_z = -1$ for ^{10}C and $T_z = 1$ for ^{10}Be.

Assuming that the 0^+_1 and 2^+_1 states of ^{10}Be belong to the same $K = 0$ rotational band, the intrinsic quadrupole moment Q_0 can be evaluated from the $\mathrm{B(E2}; 0^+_1 \rightarrow 2^+_1)$ value and the spectroscopic quadrupole moment with the following relations [49]

$$Q_0 = \frac{(I+1)(2I+3)}{3K^2 - I(I+1)} Q, \qquad (8)$$

$$Q_0 = \left[\frac{16\pi}{5} \cdot B(E2) \uparrow \right]^{1/2}, \qquad (9)$$

where Q is spectroscopic quadrupole moment, K stands for the K quantum number, and I is the angular momentum of a member of the rotational band. The intrinsic quadrupole moment evaluated by the spectroscopic quadrupole moment is 20.5 e fm^2, which is consistent to the one (21.6 e fm^2) extracted from the $\mathrm{B(E2}; 2^+_1 \rightarrow 0^+_1)$ value. This similarity seems to suggest an axially symmetric deformation in the yrast band. On the other hand, the $\mathrm{B(E2}; 2^+_2 \rightarrow 2^+_1)$ is sizable, which hints at a notable triaxial deformation of ^{10}Be. If ^{10}Be has strictly axial deformation, this B(E2) value should be hindered, as the transition between 2^+_2 state and 2^+_1 state is forbidden by the selection rule of K quantum number. The triaxiality leads to breaking of the K selection rule. For instance, $\mathrm{B(E2}; 2^+_2 \rightarrow 0^+_1)$= 0.32 e^2 fm^4 leads us to a triaxial deformation with $\gamma = 11.4^\circ$ in the Davidov-Fillipov model [50]. Thus, the present results are of interest in view of nuclear shapes, although it may be an open question as to whether the classical picture of shapes can make sense in such light nuclei. It has been discussed in [51] that ^{10}Be is triaxially deformed in a molecular-orbit calculation.

Table II shows $\mathrm{B(E2}; 2^+_2 \rightarrow 2^+_1)$ and $\mathrm{B(E2}; 2^+_2 \rightarrow 0^+_1)$ of ^{10}C too. These are considerably larger than the corresponding values of ^{10}Be. At the first glance, the triaxiality appears to be more developed in ^{10}C than in ^{10}Be.

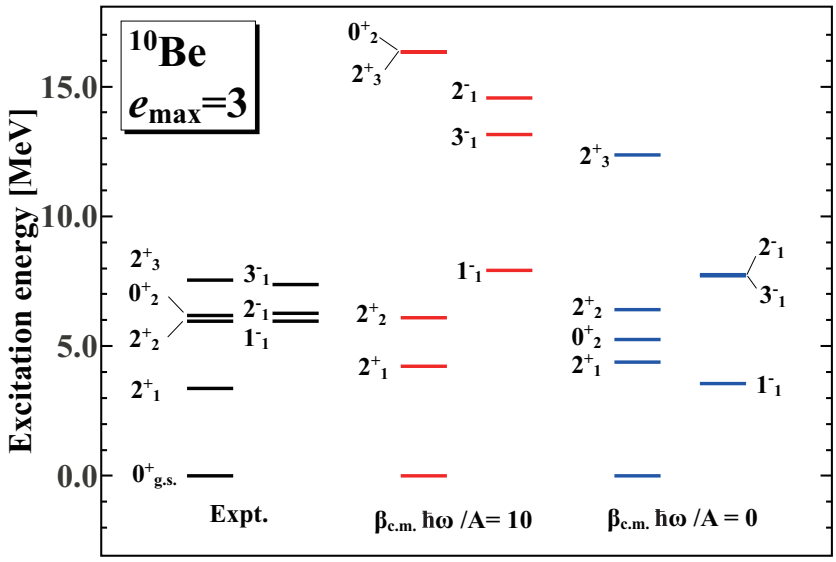

FIG. 5. (Color online) Some low-lying spectra of ^{10}Be in the $e_{\max} = 3$ model space. Black bars indicate experimental levels. Red levels are theoretical results obtained with the suppression of spurious center-of-mass motion ($\beta_{c.m.} \cdot \hbar\omega/A = 10$ MeV). Blue levels are obtained without removing the spurious center-of-mass motion.

TABLE I. B(E2) values (e^2 fm^4) of ^{10}Be obtained by NCSM with CD-Bonn and CD-Bonn 2000 potentials [11, 44], GFMC with AV18 potential and AV18 plus different three-body forces [44], AMD [41], present MCSM, and experimental [44, 45] values.

	NCSM		GFMC			AMD	MCSM	Expt.
Quantity	CD-Bonn	CDB2k	AV18	AV18+IL2	AV18+IL7			
B(E2; $2^+_1 \to 0^+_{g.s.}$)	6.58	9.8(4)	10.5(4)	8.1(3)	8.8(4)	9.46	9.29	9.2(3)
B(E2; $2^+_2 \to 0^+_{g.s.}$)	0.13	0.2(2)	3.4(2)	3.3(2)	1.8(1)		0.32	0.11(2)

But one has to be careful, as this property holds for the proton part. As the proton part and the neutron part are exchanged between the mirror nuclei ^{10}Be and ^{10}C, it can be stated that the part consisting of four protons in ^{10}Be tends to be deformed rather strongly in a prolate shape and the rest part (six neutrons) tends to be deformed in a triaxial shape, and the situation is just reversed in ^{10}C. The deformation here may be static, dynamic, in between, or even molecular [51]. Such a difference between proton and neutron sectors is quite intriguing, and experimental investigations on these theoretical findings are of much interest.

Figure 5 shows the $2^+_{1,2}$ levels calculated in two ways (a) with center-of-mass motion suppression (default setup in this paper as stated already) and (b) without it for the sake of comparison. It is found that the suppression of the spurious center-of-mass motion keeps the excitation energies of the 2^+_1 and 2^+_2 states almost unchanged. It seems that the suppression of the c.m. motion is not so relevant to these states.

On the other hand, the c.m. motion suppression is essential to the 0^+_2, 1^-_1 and 2^+_3 states, as their excitation energies are raised by several ~ 10 MeV.

It is likely that the 1^-_1 state is sensitive to spurious center-of-mass contamination. We calculate the excitation energies of 1^-_1 state of ^{10}Be with $\beta_{c.m.}\hbar\omega/A = 0, 10$ and 20 MeV. The levels are shown in Fig. 7. When changing from $\beta_{c.m.}\hbar\omega/A = 0$ to 10 MeV, the excitation energy is increased by about 4 MeV. The result with $\beta_{c.m.}\hbar\omega/A = 20$ MeV is less than 1 MeV higher, presenting a hint at convergence, although it is slower than the 2^+_1 state.

The 0^+_2 and 2^+_3 levels in Fig. 5 are lying quite high compared to the experiment. These states are expected to be intruder states with a large amount of $2p2h$ and higher excitations from the p-shell. The $e_{\max}$=3 space is considered to contain the major configurations of such intruder states, but a somewhat larger space is needed to stabilize those configurations by coupling to even higher configurations.

According to the adequacy of the $e_{\max}$=3 space, the states being discussed are divided into two groups : (i) 0^+_1 and $2^+_{1,2}$ states, (ii) 0^+_2 and 2^+_3 states. For the present interaction and nuclei, the $e_{\max}$=3 space appears to be adequate for (i), whereas is still too small for (ii). The calculated 2^-_1 and 3^-_1 levels with $\beta_{c.m.}\hbar\omega/A = 10$ MeV are higher than experimental ones in Fig. 5, although the deviations are smaller than those for 0^+_2 and 2^+_3 states. It is likely that the properties of 2^-_1 and 3^-_1 states are between the groups (i) and (ii), and should be investigated

TABLE II. $B(E2;2_1^+ \to 0_{g.s.}^+)$, $B(E2;2_2^+ \to 0_{g.s.}^+)$ and $B(E2;2_2^+ \to 2_1^+)$ values ($e^2\,fm^4$) of ^{10}Be and $B(E2;2_1^+ \to 0_{g.s.}^+)$ of the mirror nucleus ^{10}C obtained by the MCSM and the experimental data [44, 45].

	^{10}Be			^{10}C		
	$B(E2;2_1^+ \to 0_{g.s.}^+)$	$B(E2;2_2^+ \to 0_{g.s.}^+)$	$B(E2;2_2^+ \to 2_1^+)$	$B(E2;2_1^+ \to 0_{g.s.}^+)$	$B(E2;2_2^+ \to 0_{g.s.}^+)$	$B(E2;2_2^+ \to 2_1^+)$
Exp.	9.2(3)	0.11(2)		8.8(3)		
MCSM	9.29	0.32	3.28	9.30	2.15	12.81

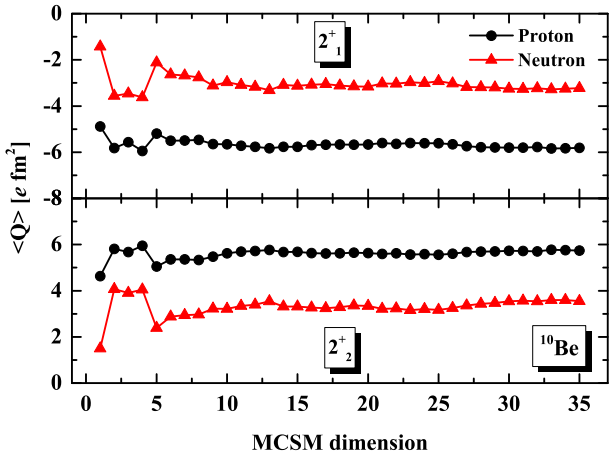

FIG. 6. (Color online) Spectroscopic quadrupole moments for protons (black circles) and neutrons (red triangles) as functions of the MCSM dimension. Upper (lower) panel is for the 2_1^+ (2_2^+) state of ^{10}Be.

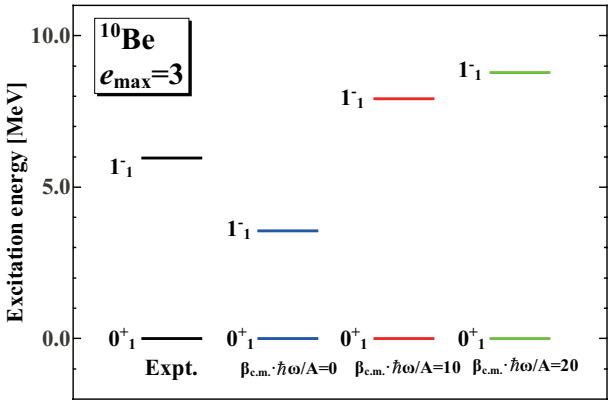

FIG. 7. (Color online) The 1_1^- excitation energy of ^{10}Be with different $\beta_{c.m.}$ values compared to the experimental data (black bars). Blue, red and green bars indicate, respectively, results with $\beta_{c.m.}\hbar\omega/A$= 0, 10 and 20 MeV.

also with wider model space.

Figure 8 indicates occupation numbers of single-particle orbits for the ground and some low-lying states of ^{10}Be. Left side is for the results without the c.m. motion suppression, whereas right side is for those with it (default setup of this work). We begin with the group (i), for which left and right sides do not show much difference. This is consistent with almost unchanged level energies of $2_{1,2}^+$ between the two corresponding calculations, as depicted in Fig. 5. Figure 8 shows that protons and neutrons are mainly in the $0s$ and $0p$ orbits. The occupation number of the $0s_{1/2}$ orbit is about 1.8 for both protons and neutrons. This value is remarkably constant for the three states in the group (i), and changes very little between proton and neutron. This means that the $0s_{1/2}$ orbit is occupied by ∼90 % probability for both proton and neutron.

If the $0s_{1/2}$ orbit is fully occupied, the ^{4}He core is ideally formed. The present result suggests that the probability of the ^{4}He-core formation is about $(0.9)^4 \sim 2/3$. The breaking of the ^{4}He core is nothing but the polarization of the core, which yields effective charges in the shell model with a core. In the present calculation, this effect is explicitly treated, producing the right amount of B(E2) values as discussed above. The UCOM transformations act on short-range part of relative-motion wave functions. Electromagnetic operator at long wave length limit is then expected to be unaffected to a large extent. Thus, we use bare charges and E2 operator, for simplicity.

The occupation number of the *sd* shell turned out to be about 0.7 for protons and neutrons combined, which corresponds approximately to the number of nucleons excited from the ^{4}He core. More precise studies on the process of effective charges will be of much interest.

For the group (ii) (0_2^+ and 2_3^+ states), the occupation numbers do change substantially between left and right sides of Fig. 8. This is consistent with the changes of their excitation energies shown in Fig. 5.

The MCSM results for ^{10}Be low-lying spectra can be compared with those of NCSM in Ref. [11]. Although the NCSM calculation does not use the same potential, the MCSM calculation shows similar results with the NCSM calculation for the 2_1^+ and 2_2^+ state. More results of the NCSM are listed and discussed in Ref. [11] for further comparison. The NCSM approach may have some difficulty for similar calculations because the full *sd* shell configurations cannot be included at $8\hbar\omega$ truncation, for instance. In the present MCSM, the *sd* configurations are fully included.

As we know from the experimental data, the 2_1^+ state of ^{12}Be has a lower excitation energy than the 2_1^+ state of ^{10}Be. This is interpreted as a phenomenon related to the evolution of the magic number in exotic nuclei. However, the present MCSM results in an e_{max}=3 model

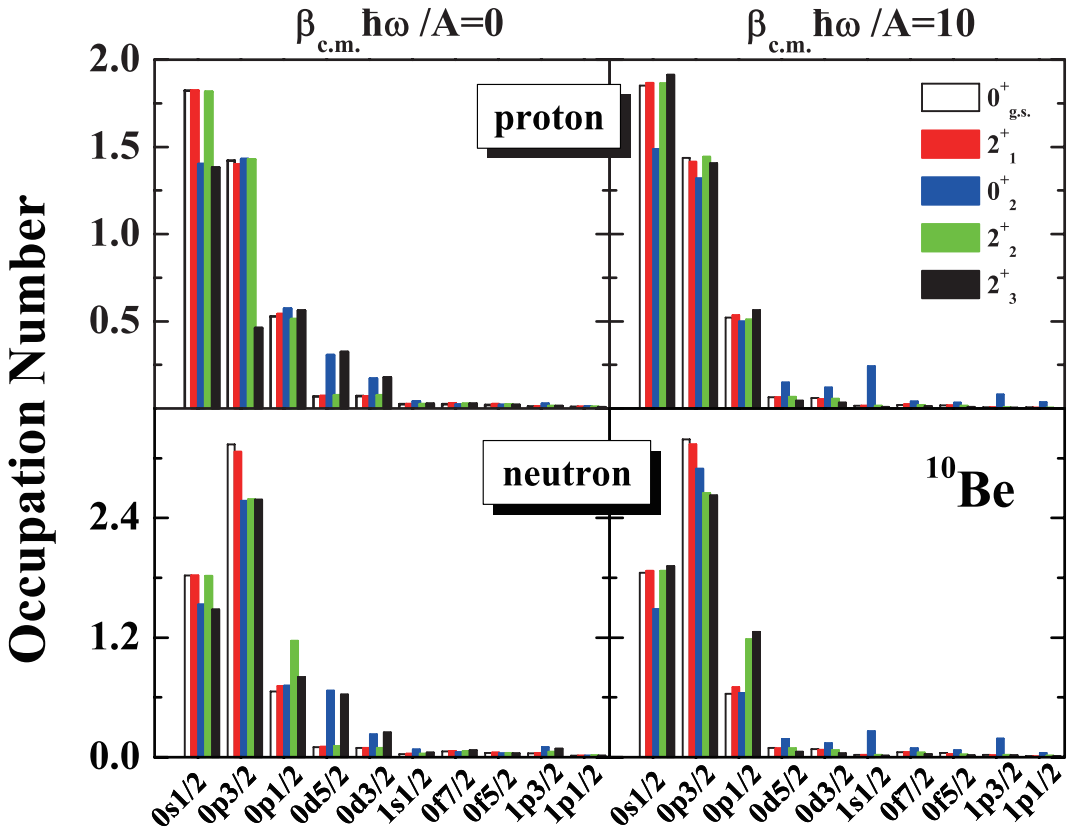

FIG. 8. (Color online) The single-particle-orbit occupation numbers of the 0^+_1 state (hollow columns), the 2^+_1 state (full red columns), the 0^+_2 state (full blue columns), the 2^+_2 state (full green columns) and the 2^+_3 state (full black columns) for ^{10}Be protons (upper panel) and neutrons (lower panel). The wave functions are calculated with $\beta_{c.m.}\hbar\omega/A$ = (a) 0 MeV and (b) 10 MeV.

space do not show this feature as can be seen in Fig. 9. The suppression of spurious c.m. motion may make the discrepancy to experiment larger. We definitely need a larger model space, and it is not tractable presently.

V. SUMMARY

For the first time, we have applied the no-core MCSM with realistic UCOM-transformed interactions to the investigation of structure of ^{10}Be and ^{12}Be.

We calculate some low-lying states of ^{10}Be and ^{12}Be in an $e_{\max}$=3 model space. The results for the 2^+_1 and 2^+_2 states of ^{10}Be show a reasonable agreement with experimental data. We have kept particular attention to the spurious center-of-mass motion, and have suppressed by Lawson's method throughout this work. The MCSM results show negative (positive) quadrupole moment for the 2^+_1 (2^+_2) state for ^{10}Be. We have analyzed the sensitivity of physical observables to center-of-mass contaminations. Some states, *e.g.*, the $2^+_{1,2}$, are stable against variations of $\beta_{c.m.}$, but others, e.g., the 1^-_1 state, are sensitive to $\beta_{c.m.}$. In fact, the suppression of spurious c.m. motion moves the 1^-_1 level by about 4 MeV to a better agreement to experiment. The obtained B(E2) values are 9.29 e^2 fm^4 for B(E2; $2^+_1 \to 0^+_{g.s.}$) for ^{10}Be and 9.30 e^2 fm^4 for its mirror nucleus ^{10}C, which are close to the experimental data with proton bare charge. Intrinsic quadrupole moments of the 2^+_1 of ^{10}Be, evaluated from the spectroscopic quadrupole moment and B(E2) value are similar to each other, suggesting an axially symmetric deformation. However, calculated B(E2; $2^+_2 \to 2^+_1$) value is sizable, being consistent with a modest triaxial deformation. The triaxial deformation is predicted to be more developed in ^{10}C, providing intriguing issues on the mirror nuclei ^{10}Be and ^{10}C to be further investigated.

The MCSM calculation presented here were performed in model spaces up to $e_{\max}$=3. Additional results, e.g.

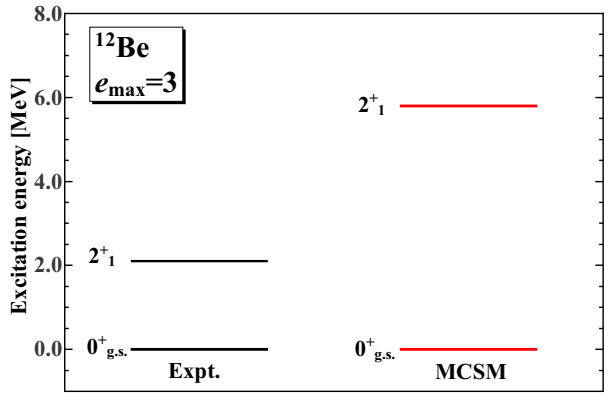

FIG. 9. (Color online) The low-lying excitation energy levels of ^{12}Be calculated by the MCSM in $e_{\max}$=3 with the UCOM potential. The black bars indicate experimental data [52], while the red bars the MCSM results with $\beta_{c.m.}\hbar\omega/A = 0$ MeV.

for ^{10}Be in $e_{\max}$=2, can be found in Ref. [43]. Although the ground-state energy of ^{10}Be is changed by about 10 MeV when going from $e_{\max}$=2 to $e_{\max}$=3, other observables turn out to be more stable already for the $e_{\max}$=3 model space. Thus, while the use of larger model spaces in the MCSM is certainly interesting and resultant changes will be evaluated in future, excitation energies and transition matrix elements look converged to a certain extent.

ACKNOWLEDGMENTS

We would like to thank Dr. Takashi Abe for discussion. One of the authors, Lang Liu, would like to thank the theoretical nuclear structure group in the University of Tokyo and Joint Center for Nuclear Physics in Peking University. This work has been supported by Grants-in-Aid for Scientific Research ((A)20244022) and for Scientific Research on Innovative Areas (20105003) from JSPS. It has also been supported by the CNS-RIKEN joint project for large-scale nuclear structure calculations. This work has also been supported by the Japanese Monbukagakusho Scholarship. R. Roth acknowledges support from the DFG (SFB 634) and from HIC for FAIR. The calculation was performed partly in Alphleet machine in CNS-RIKEN and partly in T2K super computer in the University of Tokyo.

[1] R. B. Wiringa, V. G. J. Stoks, and R. Schiavilla, Phys. Rev. C **51**, 38 (1995).
[2] R. Machleidt, Phys. Rev. C **63**, 024001 (2001).
[3] V. G. J. Stoks, R. A. M. Klomp, C. P. F. Terheggen, and J. J. de Swart, Phys. Rev. C **49**, 2950 (1994).
[4] D. R. Entem and R. Machleidt, Phys. Rev. C **68**, 041001(R) (2003).
[5] E. Epelbaum, Prog. Part. Nucl. Phys. **57**, 654 (2006).
[6] R. Machleidt and D. R. Entem, Phys. Rep. **503**, 1 (2011).
[7] S. C. Pieper and R. B. Wiringa, Annu. Rev. Nucl. Part. S. **51**, 53 (2001).
[8] S. C. Pieper, K. Varga, and R. B. Wiringa, Phys. Rev. C **66**, 044310 (2002).
[9] S. C. Pieper, Nucl. Phys. A **751**, 516 (2005).
[10] P. Navrátil, J. P. Vary, and B. R. Barrett, Phys. Rev. C **62**, 054311 (2000).
[11] E. Caurier, P. Navrátil, W. E. Ormand, and J. P. Vary, Phys. Rev. C **66**, 024314 (2002).
[12] P. Navrátil, S. Quaglioni, I. Stetcu, and B. R. Barrett, J. Phys. G: Nucl. Part. Phys. **36**, 083101 (2009).
[13] H. Feldmeier, T. Neff, R. Roth, and J. Schnack, Nucl. Phys. A **632**, 61 (1998).
[14] T. Neff and H. Feldmeier, Nucl. Phys. A **713**, 311 (2003).
[15] R. Roth, T. Neff, and H. Feldmeier, Prog. Part. Nucl. Phys. **65**, 50 (2010).
[16] R. Roth and P. Navrátil, Phys. Rev. Lett. **99**, 092501 (2007).
[17] R. Roth, H. Hergert, N. Paar, and P. Papakonstantinou, Nucl. Phys. A **788**, 12 (2007).
[18] R. Roth, Nucl. Phys. A **805**, 416c (2008).
[19] R. Roth, J. R. Gour, and P. Piecuch, Phys. Rev. C **79**, 054325 (2009).
[20] G. Puddu, J. Phys. G: Nucl. Part. Phys. **32**, 321 (2006).
[21] G. Puddu, Eur. Phys. J. A **34**, 413 (2007).
[22] S. E. Koonin, D. J. Dean, and K. Langanke, Phys. Rep. **278**, 1 (1997).
[23] M. Honma, T. Mizusaki, and T. Otsuka, Phys. Rev. Lett. **75**, 1284 (1995).
[24] T. Mizusaki, M. Honma, and T. Otsuka, Phys. Rev. C **53**, 2786 (1996).
[25] M. Honma, T. Mizusaki, and T. Otsuka, Phys. Rev. Lett. **77**, 3315 (1996).
[26] T. Otsuka, M. Honma, and T. Mizusaki, Phys. Rev. Lett. **81**, 1588 (1998).
[27] T. Otsuka, M. Honma, T. Mizusaki, N. Shimizu, and Y. Utsuno, Prog. Part. Nucl. Phys. **47**, 319 (2001).
[28] T. Mizusaki, T. Otsuka, Y. Utsuno, M. Honma, and T. Sebe, Phys. Rev. C **59**, R1846 (1999).
[29] Y. Utsuno, T. Otsuka, T. Mizusaki, and M. Honma, Phys. Rev. C **60**, 054315 (1999).
[30] N. Shimizu, T. Otsuka, T. Mizusaki, and M. Honma, Phys. Rev. Lett. **86**, 1171 (2001).
[31] T. Mizusaki, T. Otsuka, M. Honma, and B. A. Brown, Phys. Rev. C **63**, 044306 (2001).
[32] Y. Utsuno, T. Otsuka, T. Mizusaki, and M. Honma, Phys. Rev. C **64**, 011301 (2001).
[33] N. Shimizu, Y. Utsuno, T. Mizusaki, T. Otsuka, T. Abe, and M. Honma, Phys. Rev. C **82**, 061305 (2010).
[34] T. Abe, P. Maris, T. Otsuka, N. Shimizu, Y. Utsuno, and J. P. Vary, AIP Conf. Proc. **1355**, 173 (2011).
[35] T. Abe, P. Maris, T. Otsuka, N. Shimizu, Y. Utsuno, and J. P. Vary, arXiv:1204.1755v1 [nucl-th].
[36] J. Hubbard, Phys. Rev. Lett. **3**, 77 (1959).
[37] R. L. Stratonovich, Dokl. Akad. Nauk. SSSR **115**, 1097

(1957), [transl: Soviet Phys. Dokl. 2 (1957) 416].
[38] D. Gloeckner and R. Lawson, Phys. Lett. B **53**, 313 (1974).
[39] B. A. Brown and W. D. M. Rae, MSU-NSCL report (2007).
[40] R. Roth, H. Hergert, P. Papakonstantinou, T. Neff, and H. Feldmeier, Phys. Rev. C **72**, 034002 (2005).
[41] Y. Kanada-En'yo, H. Horiuchi, and A. Ono, Phys. Rev. C **52**, 628 (1995).
[42] P. Navrátil and W. E. Ormand, Phys. Rev. C **68**, 034305 (2003).
[43] L. Liu, Ph.D. thesis, the University of Tokyo (2010).
[44] E. A. McCutchan, arXiv:1201.2960v1 [nucl-ex].
[45] E. A. McCutchan, C. J. Lister, R. B. Wiringa, S. C. Pieper, D. Seweryniak, J. P. Greene, M. P. Carpenter, C. J. Chiara, R. V. F. Janssens, T. L. Khoo, T. Lauritsen, I. Stefanescu, and S. Zhu, Phys. Rev. Lett. **103**, 192501 (2009).
[46] C. Forssén, R. Roth, and P. Navrátil, arXiv:1110.0634v2 [nucl-th].
[47] G. A. Timmer, Ph.D. thesis, University of Utrecht (1976).
[48] D. E. Alburger, E. K. Warburton, A. Gallmann, and D. H. Wilkinson, Phys. Rev. **185**, 1242 (1969).
[49] A. Bohr and B. R. Mottelson, *Nuclear structure*, Vol. 2 (World Scientific, 1998).
[50] A. S. Davydov and G. F. Filippov, Nucl. Phys. **3**, 237 (1958).
[51] N. Itagaki, S. Hirose, T. Otsuka, S. Okabe, and K. Ikeda, Phys. Rev. C **65**, 044302 (2002).
[52] F. Ajzenberg-Selove, Nuclear Physics A **490**, 1 (1988).